Heterogeneity of biochar properties as a function of feedstock and production temperatures

Heterogeneity of biochars properties dependent on feedstock sources and production temperatures

Ling Zhao[a], Xinde Cao[a,] *, Ondřej Mašek[b], and Andrew Zimmerman[c]

[a] School of Environmental Science and Engineering, Shanghai Jiao Tong University, Shanghai 200240, China

[b] School of Geosciences, University of Edinburgh Kings Buildings, Edinburgh, EH9 3JN, UK

[c] Department of Geological Sciences, University of Florida, Gainesville, FL 32611, USA

[*] Corresponding author telephone: +86-021-54743926, e-mail: xdcao@sjtu.edu.cn

ABSTRACT: This study was conducted with a wide range of production temperatures (200°C–650°C) and a series of feedstock sources (n=12) to quantify the influence of these two factors on any given biochar property. The quantitative evaluation was completed using two indices, feedstock-depended heterogeneity (H_F) and temperature-depended heterogeneity (H_T), obtained from the statistic analysis of coefficient of variation. The values of H_F or H_T were positively related to the heterogeneity and correspondingly to the influence extent. Total organic carbon, fixed carbon, and mineral elements of biochars varied greatly among different feedstocks but were less affected by temperature. Biochar surface area and pH was less influenced by feedstock than by temperature, while pore volume and CEC was more affected by feedstocks than temperature. Biochar recalcitrance was mainly determined by production temperature, while potential total C sequestration depended mainly on feedstocks. CP-MAS ^{13}C NMR and FTIR showed that alkyl-C, aliphatic-C and aromatic-C was highly related to the production temperature. Raman spectroscopy revealed that distribution and state of sp^2-bonded carbon remained stable with feedstock and temperature. The results indicated that the two indices could be suitable for assessing the effect extent of feedstock source or production temperature on biochar properties.

Keywords: Biochar; Feedstock-depended heterogeneity; Temperature-depended heterogeneity; Physiochemical properties; Chemical structure

1. Introduction

Biochar, pyrogenic organic material derived from incomplete combustion of biomass, has recently received much attention due to its great potential in a wide range of environmental applications. In addition to its ability to serve as a carbon sink for mitigation of global climate change [1-3], biochar may be used as an effective contaminant sorbent [4-6] or soil nutrient amendment [7, 8]. However, the utility of each specific biochar depends upon its inherent properties. For example, biochars with high specific surface area may be used as sorbents, whereas the ones with high recalcitrance may function in carbon fixation [9]. Those rich in nutrients and minerals would be better used as soil amendments to improve fertility [10].

It has been shown that biochar characteristics are influenced by production variables such as feedstock source, heat temperature, heat duration, pyrolysis atmosphere, etc. Among these, feedstock source and heat temperature are considered to be main controls on biochar characteristics [11, 12]. For example, increases of pH, CEC, and trace metals concentration occur with increasing production temperature [13-15]. Biochars derived from wood biomasses often have higher surface area than grass biochar [15, 16]. However, most previous studies focused on a few feedstock materials or those falling into one or two categories such as crop biomasses, wood derivatives, or manures, or those made at only a few production temperatures. For example, Cantrell et al. [17] studied the impact of pyrolysis temperature and manure source on physicochemical characteristics of five manures biochar made at only two temperatures. Pereira et al. [18] investigated the labile fraction of C in biochar derived from three trees (pine, poplar and willow) at two temperatures. In general, biochars of the feedstock with the same category show similar properties compared to those made from parent material of very different types.

If we are to make use of biochar to the fullest extent of its possible applications, we must develop an understanding of its physiochemical variations for a broader range of biochar types than has previously been examined. Optimizing biochar for a specific application may require selection of a

feedstock as well as pyrolysis production technique and conditions to produce biochars with specific characteristics [19]. Thus, the objectives of this study are (i) to determine how the two main factors, feedstock source and production temperature, affect the biochar properties and (ii) to evaluate which one of the two factors dominates one property of biochar based on a series of temperatures from 200°C to 650°C and a variety of source materials (12 waste biomasses) representing 6 categories: animal manure, wood waste, crop wastes, food wastes, aquatic plants, and municipal waste. Two evaluation indices, feedstock-depended heterogeneity (H_F) and temperature-depended heterogeneity (H_T) are introduced to quantify the influence of feedstock source or production temperatures, respectively, on any given biochar property and tell which one is dominance. In this way, production materials and conditions can be chosen to produce biochars optimized for any given application. The comparison of H_F and H_T also gave a new insight to the origin and evolution of the variation properties observed among biochars.

2. Materials and Methods

2.1. Biomass Collection and Biochar Production

Twelve common waste biomasses were collected from a farm in Shanghai, China and divided into 6 categories including animal manure, wood waste, crop residue, food waste, aquatic plants, and municipal waste. The biomasses were air-dried and then ground to less than 2 mm for biochar production. Details on the production of biochar were described previously [20]. Briefly, to evaluate the feedstock source effect, all 12 ground waste biomasses were heated at 500°C under O_2-limited atmosphere for 4 h. To examine pyrolysis temperature effect, a wastes-based biochar (pig manure) and plant-based biochar (wheat straw) were chosen and pyrolyzed at 200°C, 350°C, 500°C and 650°C.

2.2. Biochar characterization

Total C analysis of biochar was conducted on an element analyzer (Vario EL III, Elementar,

German). Ash content, volatile matters (VM), and fixed carbon (FC) were determined according to standard ASTM methods [21- 23]. The metal concentrations in biochars were measured in the digestion solution using the inductively coupled plasma (ICP-AES, ICAP6000 Radial, Thermo, English), following biochar digestion using the USEPA method 3050B [24]. The cation exchange capacity (CEC) was determined according to a modified barium chloride compulsive exchange method [25]. All analyses were conducted in duplicate.

The solid phase of biochar was characterized by thermogravimetry (TG) analysis (PerkinElmer Pyris 1 TGA) with heating from 25°C to 900°C at a rate of 20°C per min. Surface functional group distributions were determined by infrared (IR) spectroscopy (IR Prestige 21 FTIR, Shimadzu, Japan) and nuclear magnetic resonance (CP-MAS ^{13}C-NMR) spectra (AVANCE III 400, Bruker, Switzerland), which were obtained at a frequency of 100.6 MHz using a Varian Unity Inova 400 NMR spectrometer. Specific surface area and pore size distribution of biochars were determined using a BET-N_2 SA analyzer (JW-BK222, Jwgb, China). Raman spectroscopy analysis was conducted using a visible Raman system (Bruker Senterra R200-L, American) with a 15 mW 532 nm He-Ne laser with excitation line set to λ_0 = 532 nm.

2.3. Calculations

Fixed Carbon (FC) of biochar was calculated as the sum of moisture, ash, and volatile matter subtracted from 100 [23].

$$\mathrm{FC\ (\%)} = 100 - \mathrm{Moisture\ (\%)} - \mathrm{Ash\ (\%)} - \mathrm{VM\ (\%)} \quad (1)$$

An index R_{50} was used to evaluate the thermal recalcitrance of biochar and was obtained by TG analysis, as recently proposed by Harvey et al [26]:

$$R_{50,biochar} = \frac{T_{50,biochar}}{T_{50,graphite}} \quad (2)$$

where $T_{50,\ biochar}$ and $T_{50,\ graphite}$ are the temperature values corresponding to 50% weight loss via oxidation/volatilization of biochar and graphite, respectively. Values are obtained directly from TG

thermograms that have been corrected for water and ash content.

Carbon sequestration potential (CS) was defined as the final carbon reserved in soil, which was calculated by subtracting the carbon lost during pyrolysis from the initial C in raw biomass, and multiplying by the recalcitrance (R_{50}) of biochar products. M was the weight of the feedstock.

$$CS(\%) = \frac{M(g)\cdot \text{Biochar yield } (\%)\cdot C\% \text{ in Biochar}\cdot R_{50}}{M(g)\cdot C\% \text{ in feedstock}} \quad (3)$$

The feedstock-depended heterogeneity (H_F) and temperature-depended heterogeneity (H_T) of biochars were calculated using the coefficient of variation (CV) in statistical method, and the larger the H_F or H_T is, the more influenced by feedstock or production temperature the biochar property is:

$$H_F \text{ or } H_T = \frac{\text{Standard deviation}}{\text{mean value}} \quad (4)$$

3. Results and Discussion

3.1. Bulk physicochemical properties

Concentrations of total carbon (TC) and fixed carbon (FC) in all 12 biochars ranged 24.2–75.8% and 3.84–72.9% with the H_F of 0.37 and 0.76 (Table 1). Increasing the temperature from 200°C to 650°C increased TC and FC (Table 1). In the temperature range, concentrations of TC and FC of the pig manure biochar were 37.0–45.3% and 12.3–42.3%, with the H_T of 0.09 and 0.48, respectively, while wheat straw biochar contained 38.7–68.9% TC and 22.5–72.1% FC, with the H_T of 0.23 and 0.41, respectively (Table 1). All H_T were lower than the H_F, indicating that TC and FC of biochars were more influenced by feedstock source than by production temperature.

Both volatile matter (VM) and weight yield were more sensitive to temperature, indicated by their higher H_T (0.5–0.81) than H_F (0.27–0.36). Kloss et al. [16] reported a similar result that labile, aliphatic compounds undergo a great loss during pyrolysis. Ash content was more sensitive to feedstock due to its higher H_F (0.53) than H_T (0.33–0.34). As shown in Table 1, ash is higher in manure and sludge biochar (18.1–42.9%), while crop residue biochar contained low ash

(2.10–7.49%). The higher ash in the manure biochar was due to richness of mineral constituents [20].

Biochars from different feedstocks had wide range minerals, while the mineral concentrations changed little with production temperature from 200°C to 650°C (Table 2). The H_F for each mineral element was higher (0.87–2.00) than H_T (0.40–0.51), indicating that mineral elements of biochars were more influenced by feedstock source than temperature. Generally, manure contained more nutrient P than crop residue and grass biochar, whereas nutrient K was higher in crop residue and grass biochar than that in manure biochar (Table 2). Thus, the utility of biochars as a soil amendment to improve soil fertility should be classified carefully according to different feedstock sources rather than production temperature.

Biochar pH varied less among the different feedstocks (8.8–10.8) than among the production temperature (5.43–10.8) (Table 1). Therefore, biochar was influenced more by temperature (H_T=0.19) than by feedstock (H_F=0.05). By contrast, the CEC varied greatly among biochars of different feedstocks (H_F=0.9) but relatively little with temperature (H_F=0.52–0.65). This may be explained that CEC is related to cations (e.g., K, Ca, Mg) which vary greatly with feedstocks (Table 2).

The physical structure of biochars, such as surface area (SA), pore volume (PV), and average pore size (APS) are typically related to its sorption and water holding capacity which, in turn, relates to its effect on soil structure, contaminant mobility, and microbial interactions. The heterogeneities of SA and APS were more related to production temperature (H_T=0.72–1.55) than feedstock (H_F=0.58–1.09), while PV was more influenced by feedstock (H_F=1.11) than temperature (H_T=0.49–0.81) (Table 1). The influence of feedstock on PV was perhaps related to the relative proportion of hemicelluloses, cellulose, and lignin fractions in biomasses. A dramatic rise in SA was observed when the temperature was increased above 350°C, at which point, cellulose is known to decompose and a phase transition from layered C to amorphous char occurs [27].

3.2. Recalcitrance and stability

The ability of biochars to resist abiotic and biotic degradation (herein referred to as recalcitrance)

144 is crucial to their success as a soil carbon sequestration. Harvey et al (2012) have developed an index
145 (R_{50}) to evaluate the recalcitrance of biochars, which uses the energy required for thermal oxidation
146 of the biochars (normalized to that for oxidation of graphite) as a measure of recalcitrance [26].
147 The water and ash content-corrected thermogravimetry patterns of biochars are presented in Fig.
148 1. The temperatures at which 50% biochar weight loss occurred ranged within 614–727^{o}C for all
149 feedstocks and within 338–767^{o}C for all production temperature of pig manure biochar and wheat
150 straw biochar. The calculated R_{50} for biochars from all feedstocks fell in a narrow range of 0.69–0.82,
151 with H_F being 0.06, while R_{50} for biochars produced at 200^{o}C–650^{o}C was within a wide range of
152 0.38–0.87, with H_T being 0.29–0.34 (Table 1), indicating that the recalcitrance of biochar was mainly
153 determined by production temperature, which was also expected from previous findings [9]. Biochar
154 recalcitrance is related to aromatic C which increased with increasing temperature, regardless of
155 nature of feedstocks (shown below). Fig. 1 also shows that all biochars produced at same temperature
156 had similar R_{50} and the gap among different feedstocks enlarged with the increase of production
157 temperature, further suggesting that temperature was the dominating control on recalcitrance.
158 Carbon sequestration potential (CS) was evaluated assisted by R_{50} as shown in equation 3. CS of
159 all 12 biochars ranged 23.7–54.0% with H_F being 0.27, while those for pig manure biochar and
160 wheat straw biochar at production temperature of 200^{o}C–650^{o}C were 33.1–38.4% and 34.3–44.6%,
161 respectively, with H_T being 0.07 and 0.11, respectively. The H_T was lower than H_F, indicating that
162 temperature had less influence on the carbon sequestration capacity. It is probably that low
163 production temperature could retain much C in biochar, but a considerable amount of these C would
164 be abiotically or microbially mineralized [9, 28]; when the temperature increases, more C would lose
165 in pyrolysis, but more recalcitrant C would be produced [29]. The contradictory effects would keep
166 biochar-C less changed. Therefore, the C sequestration was mainly determined by the inherent
167 molecular configuration of biomasses [30].
168 *3.3. Biochar chemical structure*

169 The carbon cluster size and functional group distributions were identified by CP-MAS ^{13}C NMR
170 and FTIR, and are shown in Fig. 2 and 3, respectively. The ^{13}C NMR spectrograms of biochars from
171 12 feedstocks were very similar, whereas they varied greatly among those produced from a single
172 feedstock type across a range of temperatures (Fig. 2). Table 3 summarizes the relative proportion of
173 C in each chemical functional groups for the biochars examined, which were integrated in the
174 chemical shift (ppm) resonance intervals of 0–46, 46–65, 65–90, 90–108, 108–145, 145–160,
175 160–185, 185–225 ppm [31]. Clearly, aromatic C with chemical shift of 108–145 ppm was the main
176 C-containing functional group in all biochars (45.0–80.3%), with an H_F of being 0.15. The aromatic
177 C in biochars increased from 2.24% at 200^{o}C to 62.9% at 650^{o}C with H_T being 0.68 (Table 3).
178 Therefore, the aromatic C was mainly controlled by the production temperature, agreeing with the
179 recalcitrance shown above.
180 The control of aromatic content by production temperature, as opposed to feedstock type, was
181 true for other C-containing functional groups. For example, the subdominant abundance of C was
182 alkyl C (mainly CH_2 and CH_3 sp^3 carbons) at the chemical shift of 0–46 ppm accounted for
183 10.9–18.6% of the C-containing functional groups in biochars of different feedstocks at production
184 temperature 500^{o}C (H_F =0.15) and for 3.17–38.8% in biochars of different temperatures (H_T =0.90).
185 The 200^{o}C biochars retained properties like the raw materials. For example, the C within 46–65 ppm
186 and 65–90 ppm, representing methoxy and N alkyl C from OCH_3, C–N and complex aliphatic
187 carbons, respectively, as well as O-alkyl C was in high proportions.
188 The FTIR spectra also indicate a range of superficial functional groups among different biochars
189 (Fig. 3). The absorption peaks at 2916 cm^{-1} are assigned to saturated C-H stretching vibration
190 (aliphatic C-H), and a wide absorption peak at 3200–3500 cm^{-1} is attributed to –OH stretching [20].
191 These peaks existed in all biomasses, while disappeared above 350^{o}C, which were influenced more
192 by temperature indicating the dehydration of cellulosic and ligneous components (Fig. 3 c and d).
193 The peaks at 1465–1340 cm^{-1} are saturated C-H bending vibration and it is of great difference among

biochars of feedstocks, while less difference among biochars produced at different temperatures. The –COO anti-symmetric stretching of amino acids (1574 and 1600 cm^{-1}) appeared in wood and crop waste biochars, which presented little change until the temperature rose to 650°C. The intensity of C=O stretching of aromatic rings (1593 cm^{-1}) decreased with temperature rise and seemed similar in all feedstocks. Peaks at 874 and 1034 cm^{-1} were assigned to the bands of the out-of-plane bending for CO_3^{2-}, which exists more in biochars of wastes and manures and less in plant-based biochars, and was less influenced by production temperature [32, 33]. The NMR and FTIR results all showed the aromatization among different feedstocks and production temperature [34]. The recalcitrance and C sequestration have close relationship with carbon configuration, which perhaps determines the breakdown of C-bond and re-aggregation of C cluster under heat treatment [35].

Raman spectroscopy has been widely used to evaluate the microstructure of carbon materials, particularly the distribution and state of sp^2-bonded (aromatic) carbon [36], which is embedded in a disordered and amorphous matrix of both sp^3 and sp^2 carbon. The G-band centered at 1580 cm^{-1} arises from the in-plane vibrations of the sp^2-bonded crystallite carbon and has been observed for single crystal graphite, while another peak denoted as the "disorder" peak (or D-band) centered at 1357 cm^{-1} is typically observed in polycrystalline graphite. The D-band is attributed to in-plane vibrations of sp^2-bonded carbon within structural defects. For disordered carbon materials the ratio of the integrated intensities I_D/I_G is often reported to be inversely proportional to the lateral extension La of the graphene materials [37].

As shown in Fig. 4a and b, both G-band and D-band appeared in all 12 biochars with production temperature of 500°C and had the similar I_D/I_G (0.804–1.51), with low H_F (0.31) (Table 1), implying that ratio of disordered or strongly distorted structure of turbostratic carbon to ordered graphite crystals was less determined by feedstocks than production temperature. For biochars produced at a range of production temperature, bands were found to develop at 350°C, indicating the beginning of aromatization. The increase of I_D/I_G with temperature increasing from 350°C to 650°C was also not

219 obvious (H_T <0.36) since the temperature used in this study was in a relatively low range and their
220 influence on biochar microstructure could be negligible.

221 **4. Conclusions**

222 Biochars of different physical and chemical properties will be more suited for one application or
223 another, e.g. soil amelioration, C sequestration, contaminant remediation, etc. The biochar properties
224 have been shown to be mainly controlled by feedstock source and production temperature. The
225 relationship between H_F and H_T for a range of properties in the biochar examined is depicted in Fig.
226 5. Biochar yield, pH, recalcitrance, and volatile matter plotted above the 1:1 line, indicating that
227 these properties are controlled more strongly by production temperature. Thus, any application of
228 biochar related to these properties would call for greater attention to the production temperature. For
229 example, if a biochar is produced for carbon sequestration purpose, high temperature is required
230 since it increases recalcitrance. If a biochar is intended for use as adsorption sorbent, increasing
231 temperature (>500^{o}C) would improve the surface area and micropore volume. However, feedstock
232 should be also considered, since H_F was also high (Fig. 5). Biochar C, CEC, fixed C, carbon
233 sequestration, mineral concentrations, and ash content plotted below the 1:1 line (Fig. 5), indicating
234 that these properties are controlled more strongly by feedstock sources. Therefore, any application of
235 biochar related to these properties should focus on raw materials selection. If a biochar is prepared as
236 soil amendment, biomass rich in minerals would be advisable. For example, pig manures and aquatic
237 plant biochars contain abundant P, K, Ca, Mg, etc (Table 2).

238 Overall, the results obtained from this study indicate that feedstock source or production
239 temperature affect biochar properties to different degrees and consideration of production conditions
240 guide the development of 'optimum' biochars for different environmental applications

241

242

243

Acknowledgements

This work was in part supported by the National Natural Science Foundation of China (NO. 21077072, 21107070), Shanghai Pujiang Talent Project (11PJ1404600), and the University Innovation Project (AE1600004).

249 **References**

250 [1] T. Whitman, C.F. Nicholson, D. Torres, J. Lehmann, Climate change impact of biochar cook
251 stoves in western Kenyan farm households: System dynamics model analysis, Environ. Sci.
252 Technol. 45 (2011) 3687–3694.
253 [2] D. Matovic, Biochar as a viable carbon sequestration option: Global and Canadian perspective,
254 Energy 36 (2011) 2011–2016.
255 [3] K.G. Roberts, B.A. Gloy, S. Joseph, N.R. Scott, J. Lehmann, Life cycle assessment
256 of biochar systems: Estimating the energetic, economic, and climate change potential, Environ.
257 Sci. Technol. 44 (2010) 827–833.
258 [4] X.D. Cao, L. Ma, B. Gao, W. Harris, Dairy-manure derived biochar effectively sorbs lead and
259 atrazine, Environ. Sci. Technol. 43 (2009) 3285–3291.
260 [5] B.L. Chen, D.D. Zhou, L.Z. Zhu, Transitional adsorption and partition of nonpolar and polar
261 aromatic contaminants by biochars of pine needles with different pyrolytic temperatures, Environ.
262 Sci. Technol. 42 (2008) 5137–5143.
263 [6] H.L. Lu, W.H. Zhang, Y.X. Yang, X.F. Huang, S.Z. Wang, R.L. Qiu, Relative distribution of
264 Pb^{2+} sorption mechanisms by sludge-derived biochar, Water Res. 46 (2012) 854–862.
265 [7] C.J. Atkinson, J.D. Fitzgerald, N.A. Hipps, Potential mechanisms for achieving agricultural
266 benefits from biochar application to temperate soils: a review, Plant Soil 337 (2010) 1–18.
267 [8] M.K. Hossain, V. Strezov, K.Y. Chan, P.F. Nelson, Agronomic properties of wastewater sludge
268 biochar and bioavailability of metals in production of cherry tomato (Lycopersicon esculentum),
269 Chemosphere 78 (2010) 1167–1171.
270 [9] A.R. Zimmerman, Abiotic and microbial oxidation of laboratory-produced lack carbon (Biochar),
271 Environ. Sci. Technol. 44 (2010) 1295–1301.
272 [10] E.R. Graber, Y.M. Harel, M. Kolton, E. Cytryn, A. Silber, D.R. David, L. Tsechansky, M.
273 Borenshtein, Y. Elad, Biochar impact on development and productivity of pepper and tomato

grown in fertigated soilless media, Plant Soil 337 (2010) 481–496.

[11] M.I. Bird, C.M. Wurster, P.H. de Paula Silva, A.M. Bass, R. de Nys, Algal biochar–production and properties, Bioresour. Technol. 102 (2010) 1886–1891.

[12] A. Enders, K. Hanley, T. Whitman, S. Joseph, J. Lehmann, Characterization of biochars to evaluate recalcitrance and agronomic performance, Bioresour. Technol. 114 (2012) 644–653.

[13] M.K. Hossain, V. Strezov, K.Y. Chan, A. Ziolkowski, P.F. Nelson, Influence of pyrolysis temperature on production and nutrient properties of wastewater sludge biochar, J. Environ. Manage. 92 (2011) 223–228.

[14] J.H. Yuan, R.K. Xu, H. Zhang, The forms of alkalis in the biochar produced from crop residues at different temperatures, Bioresour. Technol. 102 (2011) 3488–3497.

[15] A. Mukherjee, A.R. Zimmerman, W. Harris, Surface chemistry variations among a series of laboratory-produced biochars, Geoderma 163 (2011) 247–255.

[16] S. Kloss, F. Zehetner, A. Dellantonio, R. Hamid, F. Ottner, V. Liedtke, M. Schwanninger, M.H. Gerzabek, G. Soja, Characterization of slow pyrolysis biochars: effects of feedstocks and pyrolysis temperature on biochar properties, J. Environ. Qual. 41 (2012) 990–1000.

[17] K.B. Cantrell, P.G. Hunt, M. Uchimiya, J.M. Novak, K.S. Ro, Impact of pyrolysis temperature and manure source on physicochemical characteristics of biochar, Bioresour. Technol. 107 (2012) 419–428.

[18] R.C. Pereira, J. Kaal, M.C. Arbestain, R.P. Lorenzo, W. Aitkenhead, M. Hedley, F. Macías, J. Hindmarsh, J.A. Maciá-Agulló, Contribution to characterisation of biochar to estimate the labile fraction of carbon, Org. Geochem. 42 (2011) 1331–1342.

[19] J.A. Ippolito, D.A. Laird, W.J. Busscher, Environmental Benefits of Biochar, J. Environ. Qual. 41 (2012) 967–972.

[20] X.D. Cao, W. Harris, Properties of dairy-manure-derived biochar pertinent to its potential use in remediation, Bioresour. Technol. 101 (2010) 5222–5228.

299 [21] Standard test method for ash in the analysis sample of coal and coke from coal. Designation:
300 D3174–11. ASTM Committee, 2011.
301 [22] Standard test method for volatile matter in the analysis sample of coal and coke. Designation:
302 D3175–11. ASTM Committee, 2007.
303 [23] Standard practice for proximate analysis of coal and coke. Designation: D3172–07a. ASTM
304 Committee, 2007.
305 [24] U.S.Environmental Protection Agency (USEPA), Test methods for evaluating solid waste,
306 Laboratory Manual Physical/Chemical Methods. U.S. Gov. Print Office, Washington, DC. 1986.
307 [25] J.W. Lee, M. Kidder, B.R. Evans, S. Paik, A.C. Buchanan, C.T. Garten, R.C. Brown,
308 Characterization of biochars produced from cornstovers for soil amendment, Environ. Sci.
309 Technol. 44 (2010) 7970–7974.
310 [26] O.R. Harvey, L.J. Kuo, A.R. Zimmerman, P. Louchouarn, J.E. Amonette, B.E. Herbert, An
311 index-based approach to assessing recalcitrance and soil carbon sequestration potential of
312 engineered black carbons (Biochars), Environ. Sci. Technol. 46 (2012) 1415−1421.
313 [27] K.Y. Chan, L. van Zwieten, I. Meszaros, A. Downie, S. Joseph, Agronomic values of greenwaste
314 biochar as a soil amendment, Austra. J. Soil Res. 45 (2007) 629–634.
315 [28] C.H. Cheng, J. Lehmann, J.E. Thies, S.D. Burton, M.H. Engelhard, Oxidation of black carbon
316 by biotic and abiotic processes, Org. Geochem. 37 (2006) 1477−1488.
317 [29] N. Worasuwannarak, T. Sonobe, W. Tanthapanichakoon, Pyrolysis behaviors of rice straw, rice
318 husk, and corncob by TG-MS technique, J. Anal. Appl. Pyrolysis. 78 (2007) 265–271.
319 [30] Mašek, O., Brownsort, P., Cross, A., Sohi, S., 2011. Influence of production conditions on the
320 yield and environmental stability of biochar. Fuel (In press, doi:10.1016/j.fuel.2011.08.044).
321 [31] K. Jindo, K. Suto, K. Matsumoto, C. García, T. Sonoki, M.A. Sanchez-Monedero, Chemical and
322 biochemical characterisation of biochar-blended composts prepared from poultry manure,
323 Bioresour. Technol. 110 (2012) 396–404.

[32] L. Beesley, E. Moreno-Jiménez, J.L. Gomez-Eyles, Effects of biochar and greenwaste compost amendments on mobility, bioavailability and toxicity of inorganic and organic contaminants in a multi-element polluted soil, Environ. Pollut. 158 (2010) 2282–2287.

[33] B. Singh, B.P. Singh, A.L. Cowie, Characterisation and evaluation of biochars for their application as a soil amendment, Austra. J. Soil Res. 48 (2010) 516–525.

[34] M. Keiluweit, P.S. Nico, M.G. Johnson, M. Kleber, Dynamic molecular structure of plant biomass-derived black carbon (Biochar), Environ. Sci. Technol. 44 (2010) 1247–1253

[35] B.T. Nguyen, J. Lehmann, W.C. Hockaday, S. Joseph, C.A. Masiello, Temperature sensitivity of black carbon decomposition and oxidation, Environ. Sci. Technol. 44 (2010) 3324–3331.

[36] Y.R. Rhim, D.J. Zhang, D.H. Fairbrother, K.A. Wepasnick, K.J. Livi, R.J. Bodnar, D.C. Nagle, Changes in electrical and microstructural properties of microcrystalline cellulose as function of carbonization temperature, Carbon 48 (2010) 1012–1024.

[37] O. Paris, C. Zollfrank, G.A. Zickler, Decomposition and carbonisation of wood biopolymers-a microstructural study of softwood pyrolysis, Carbon 43 (2005) 53–66.

Table 1

Compositions, physico-chemical properties, and structural characteristics of biochars derived from 12 waste biomasses produced at 500°C and biochars produced from pig manure and wheat straw at 200°C–650°C.

Biochar feedstock	Temperature[a]	**OC[b] (%)**	**FC[c] (%)**	**CS[d] (%)**	**Yield (%)**	**VM[e] (%)**	**Ash (%)**	**pH**	**CEC[f] (cmol·kg^{-1})**	**SA[g] (m^2·g^{-1})**	**PV[h] (cm^3·g^{-1})**	**APS[i] (nm)**	**R_{50}[j]**	**I_D/I_G[k]**
Cow manure	500°C	43.7	14.7	52.5	57.2	17.2	67.5	10.2	149	21.9	0.028	5.04	0.72	1.09
Pig manure		42.7	40.2	33.1	38.5	11.0	48.4	10.5	82.8	47.4	0.075	6.35	0.74	1.19
Shrimp hull		52.1	18.9	32.4	33.4	26.6	53.8	10.3	389	13.3	0.039	11.6	0.78	1.51
Bone dregs		24.2	10.5	28.3	48.7	11.0	77.6	9.57	87.9	113	0.278	9.86	0.82	1.15
Wastewater sludge		26.6	20.6	23.7	45.9	15.8	61.9	8.82	168	71.6	0.060	3.37	0.76	-
Waste paper		56.0	16.4	28.3	36.6	30.0	53.5	9.88	516	133	0.084	2.51	0.80	1.29
Sawdust		75.8	72.0	31.1	28.3	17.5	9.94	10.5	41.7	203	0.125	2.23	0.73	1.33
Grass		62.1	59.2	27.7	27.8	18.9	20.8	10.2	84.0	3.33	0.010	11.9	0.70	1.20
Wheat straw		62.9	63.7	34.4	29.8	17.6	18.0	10.2	95.5	33.2	0.051	6.10	0.71	1.10
Peanut shell		73.7	72.9	39.1	32.0	16.0	10.6	10.5	44.5	43.5	0.040	3.72	0.69	1.15
Chlorella		39.3	17.4	35.3	40.2	29.3	52.6	10.8	562	2.78	0.010	15.0	0.77	1.16
Waterweeds		25.6	3.84	54.0	58.4	32.4	63.5	10.3	509	3.78	0.009	9.52	0.78	0.80
	H_F[l]	0.37	0.76	0.27	0.27	0.36	0.53	0.05	0.90	1.09	1.11	0.58	0.06	0.31
Pig manure	200°C	37.0	12.6	38.4	98.0	50.7	35.7	8.22	23.6	3.59	-	-	0.39	-
	350°C	39.1	34.7	33.6	57.5	27.4	37.2	9.65	49.0	4.26	0.024	12.8	0.55	0.56
	500°C	42.7	40.2	33.1	38.5	11.0	48.4	10.5	82.8	47.4	0.075	6.35	0.74	1.19
	650°C	45.3	19.2	34.4	35.8	10.7	69.6	10.8	132	42.4	0.062	5.80	0.78	0.90
	H_T[m]	0.09	0.48	0.07	0.50	0.76	0.33	0.12	0.65	0.97	0.49	0.47	0.29	0.36
Wheat straw	200°C	38.7	22.5	37.7	99.3	70.2	7.21	5.43	32.1	2.53	-	-	0.38	-
	350°C	59.8	53.2	44.6	52.5	31.3	14.7	8.69	87.2	3.48	0.010	11.3	0.55	1.24
	500°C	62.9	63.7	34.3	29.8	17.6	18.0	10.2	95.5	33.2	0.051	6.10	0.71	1.16
	650°C	68.9	72.1	41.5	26.8	11.1	16.2	10.2	146	182	0.093	2.05	0.87	1.32
	H_T	0.23	0.41	0.11	0.64	0.81	0.34	0.26	0.52	1.55	0.808	0.72	0.34	0.06

[a] Biochar production temperature
[b] Organic carbon
[c] FC is fixed carbon (%, dry basis)
[d] CS is potential carbon sequestration (%) after pyrolysis and mineralization
e VM is volatile matter (%, dry basis)
f CEC is cation exchange capacity ($cmol \cdot kg^{-1}$)
g SA is BET-N_2 surface area ($m^2 \cdot g^{-1}$)
h PV is pore volume ($cm^3 \cdot g^{-1}$)
i APS is average pore diameter (nm)
[j] R_{50} is a novel index for evaluating biochar recalcitrance derived from thermogravimetric data (Harvey et al., 2011)
[k] I_D/I_G, Ratio of D-band and G-band from Raman spectra
[l] H_F, feedstock-dependant heterogeneity index (see text)
[m] H_T, temperature-dependant heterogeneity index (see text)

Table 2

Mineral constituents ($g \cdot kg^{-1}$) of biochars derived from 12 waste biomasses produced at 500°C and biochars produced from pig manure and wheat straw at 200°C–650°C.

Biochar feedstock	**T**emperature [a]	**P**	**K**	**Ca**	**Mg**	**Cu**	**Zn**	**Al**	**Fe**	**Mn**
Cow manure	500°C	0.646	1.021	3.795	1.569	0.013	0.052	0.506	0.616	0.044
Pig manure		4.386	3.560	3.474	2.801	0.078	0.101	0.455	0.696	0.123
Shrimp hull		2.585	1.896	21.03	0.590	0.013	0.015	0.024	0.023	0.006
Bone dregs		10.86	0.444	31.82	0.508	0.001	0.016	0.010	0.009	0.001
Wastewater sludge		1.702	0.525	6.573	0.645	0.038	0.152	1.929	2.209	0.045
Waste paper		0.124	0.079	22.84	0.584	0.001	0.010	0.361	0.455	0.008
Sawdust		0.061	1.189	2.290	0.348	0.001	0.010	0.097	0.168	0.009
Grass		0.590	5.151	5.236	0.530	0.003	0.023	0.109	0.152	0.011
Wheat straw		0.074	5.182	0.954	0.297	0.001	0.002	0.047	0.074	0.007
Peanut shell		0.166	1.733	1.338	0.458	0.002	0.003	0.218	0.256	0.018
Chlorella		0.717	13.67	17.50	0.779	0.003	0.012	0.547	0.409	0.912
Waterweeds		0.514	3.224	23.13	0.663	0.002	0.010	0.685	0.559	1.025
	H_F [b]	1.66	1.19	0.93	0.87	1.78	1.37	1.27	1.27	2.00
Pig manure	200°C	1.72	1.40	1.36	1.10	0.031	0.040	0.179	0.273	0.048
	350°C	2.94	2.38	2.33	1.88	0.052	0.068	0.305	0.466	0.082
	500°C	4.39	3.56	3.47	2.80	0.078	0.101	0.455	0.696	0.123
	650°C	4.72	3.83	3.74	3.02	0.084	0.109	0.490	0.749	0.132
	H_T [c]	0.40	0.40	0.40	0.40	0.40	0.40	0.40	0.40	0.40
Wheat straw	200°C	0.022	1.55	0.286	0.089	0.000	0.001	0.014	0.022	0.002
	350°C	0.042	2.94	0.540	0.168	0.001	0.001	0.027	0.042	0.004
	500°C	0.074	5.18	0.95	0.297	0.001	0.002	0.047	0.074	0.007
	650°C	0.082	5.75	1.06	0.329	0.001	0.002	0.052	0.082	0.008
	H_T	0.51	0.51	0.51	0.51	0.51	0.51	0.51	0.51	0.51

[a] Biochar production temperature
[b] H_F, Feedstock-depended heterogeneity (see text)
[c] H_T, Temperature-depended heterogeneity (see text)

Table 3

Relative proportion (% of biochar-C) of chemical functional groups in biochars derived from 12 feedstocks at 500°C and biochars produced from pig manure and wheat straw at 200°C–650°C, determined by CP-MAS ^{13}C NMR.

Biochar feedstock	Temperature [a]	Chemical shift (ppm), δ								
		0-46	46-65	65-90	90-108	108-145	145-160	160-185	185-225	225-250
Cow manure	500°C	10.87	-	-	3.59	61.4	7.68	4.79	6.48	6.58
Pig manure		11.7	2.9	16.0	4.20	45.0	2.80	18.6	0.40	-
Shrimp hull		12.7	1.9	2.50	6.00	75.0	4.10	-	-	1.90
Bone dregs		13.4	-	1.20	7.58	72.9	4.89	0.30	-	1.10
Wastewater sludge		18.6	1.5	5.10	5.90	63.4	5.30	-	0.70	1.90
Waste paper		13.7	-	0.20	2.49	75.0	5.28	-	-	5.18
Sawdust		12.4	-	1.00	2.29	78.3	2.89	-	-	5.08
Grass		11.0	0.00	0.00	2.50	80.3	2.79	0.30	-	4.29
Wheat straw		12.6	-	-	1.30	79.1	3.49	-	0.90	4.39
Peanut shell		12.5	0.80	-	1.60	79.6	3.90	-	-	3.90
Chlorella		13.4	0.60	1.30	3.70	77.3	2.80	-	-	3.90
Waterweeds		12.4	2.50	0.10	10.4	65.7	4.00	-	0.70	4.60
	H_F [b]	0.15	1.85	2.20	0.63	0.15	0.35	5.62	8.37	0.65
Pig manure	200°C	38.8	20.6	27.8	5.37	2.79	0.60	7.56	-	-
	350°C	38.3	5.74	11.3	6.82	34.7	3.80	7.98	-	-
	500°C	11.7	2.9	16.0	4.20	45.0	2.80	18.6	0.40	-
	650°C	3.17	-	1.29	7.14	57.6	3.17	1.78	11.5	14.7
	H_T [c]	0.80	1.28	0.78	0.23	0.67	0.54	0.78	5.51	4.44
Wheat straw	200°C	3.77	13.3	66.9	14.0	1.69	0.89	-	-	-
	350°C	33.7	4.59	0.80	3.59	49.4	7.98	0.10	-	0.40
	500°C	12.6	-	-	1.30	79.1	3.49	-	0.90	4.39
	650°C	5.47	1.00	3.18	6.17	68.2	4.78	3.68	4.28	3.28
	H_T	0.99	1.33	1.87	0.88	0.69	0.69	3.05	1.96	1.10

[a] Biochar production temperature

[b] H_F, Feedstock-depended heterogeneity

[c] H_T, Temperature-depended heterogeneity

Note: The spectra were integrated in the chemical shift (ppm) resonance intervals of 0–46 ppm (alkyl C, mainly CH_2 and CH_3 sp^3 carbons), 46–65 ppm (methoxy and N alkyl C from OCH_3, C–N and complex aliphatic carbons), 65–90 ppm (O-alkyl C, such as alcohols and ethers), 90–108 ppm (anomeric carbons in carbohydrate-like structures), 108–145 ppm (aromatic and phenolic carbon), 145–160 ppm (Oxygen aromatic carbon and olefinic sp^2 carbons), 160–185 ppm (carboxyl, amides and ester) and 185–225 ppm (carbonyls).

Figure Captions

FIGURE 1. Corrected thermogravimetry patterns of biochars derived from 12 feedstocks at 500°C (a) and biochar produced from pig manure and wheat straw at 200°C–650°C (b).

FIGURE 2. CP-MAS ^{13}C NMR spectrogram of biochars derived from 12 feedstocks at 500°C (a, b) and biochar produced from pig manure (c), and wheat straw at 200°C–650°C (d). 1. Cow manure, 2. Pig manure; 3. Shrimp hull; 4. Bone dregs; 5. Wastewater sludge; 6. Waste paper; 7. Sawdust; 8. Grass; 9. Wheat straw; 10. Peanut shell; 11. Chlorella; 12. Waterweeds.

FIGURE 3. FTIR spectra of biochars derived from 12 feedstocks at 500°C (a, b) and biochars produced from pig manure (c) and wheat straw at production temperature ranging 200°C–650°C (d).

FIGURE 4. Raman spectra of biochars derived from 12 feedstocks at 500°C (a, b) and biochars produced from pig manure (c) and wheat straw at production temperature ranging 200°C–650°C (d).

FIGURE 5. Comparison of feedstock-depended heterogeneity (H_F) and temperature-depended heterogeneity (H_T) for different properties of biochar. See Table 1 for abbreviation.

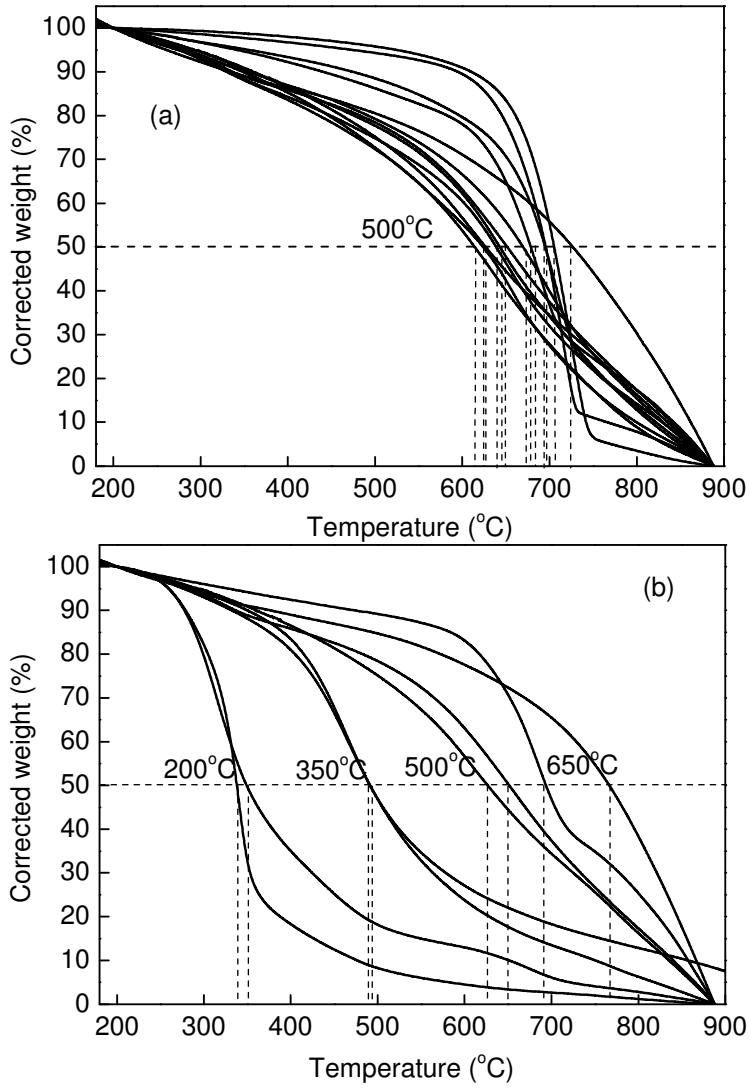

Fig. 1. Corrected thermogravimetric curves for biochars derived from12 feedstocks at HTT of 500°C (a) and biochar produced from pig manure and wheat straw at HTT 200°C–650°C (b).

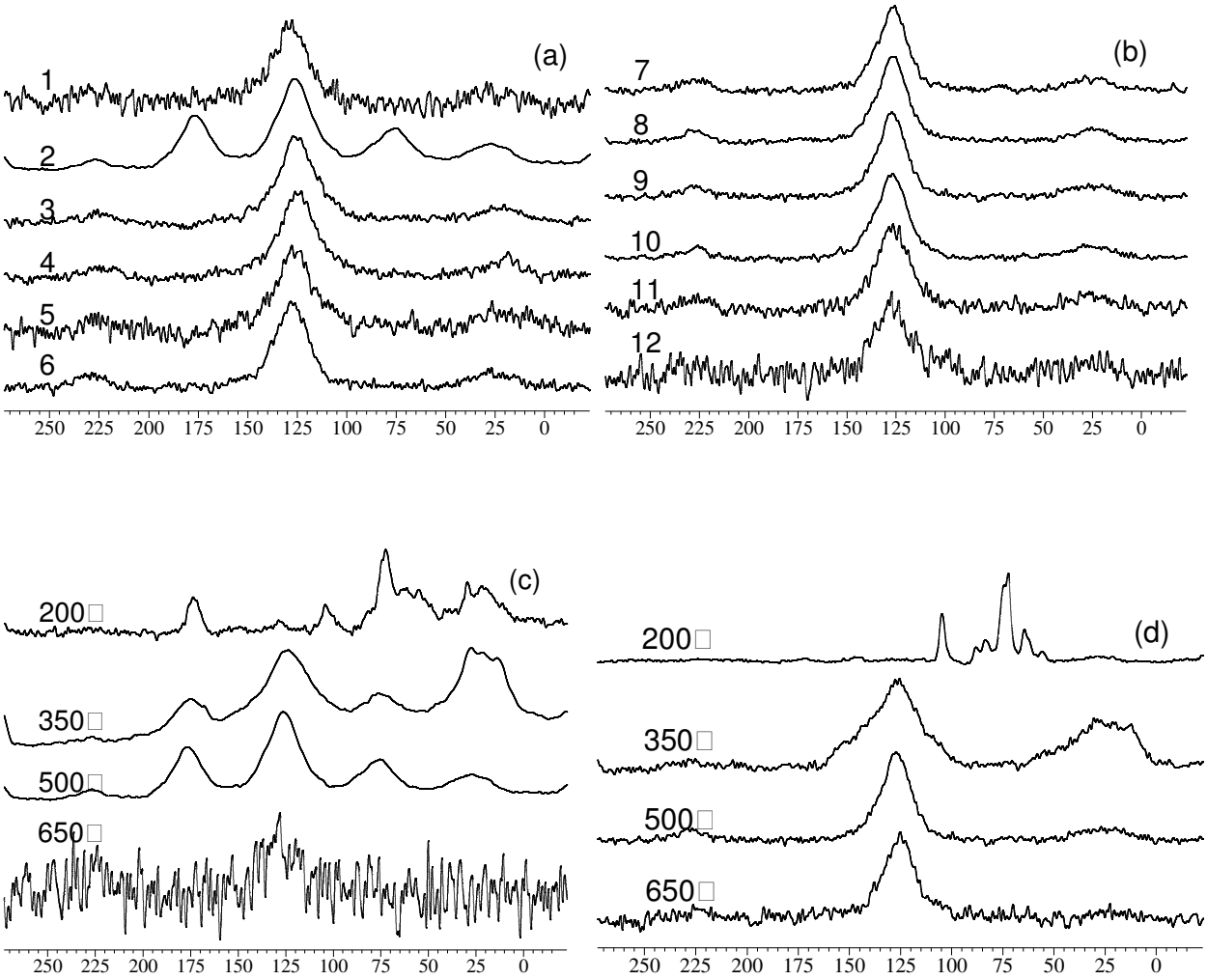

Fig. 2. CP-MAS ^{13}C NMR spectrogram for biochars derived from 12 feedstocks at HTT 500^{o}C (a, b) and for biochar produced from pig manure (c), and wheat straw at HTT ranging 200^{o}C–650^{o}C (d). 1. Cow manure, 2. Pig manure; 3. Shrimp hull; 4. Bone dregs; 5. Wastewater sludge; 6. Waste paper; 7. Sawdust; 8. Grass; 9. Wheat straw; 10. Peanut shell; 11. Chlorella algae; 12. Waterweeds.

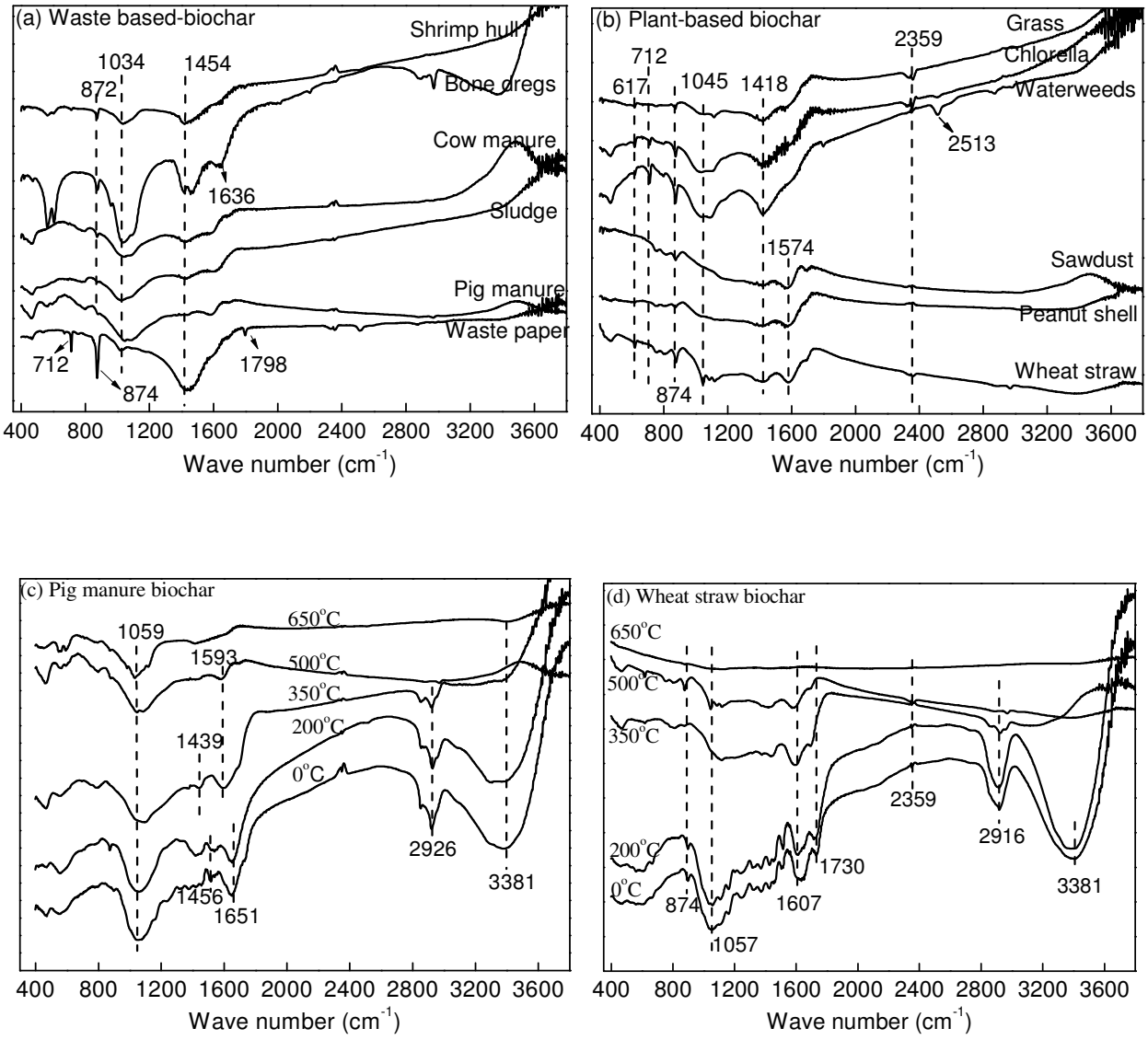

Fig. 3. FTIR spectra of biochars derived from 12 feedstocks at 500°C (a, b) and biochars produced from pig manure (c) and wheat straw (d) at production temperature ranging 200°C–650°C.

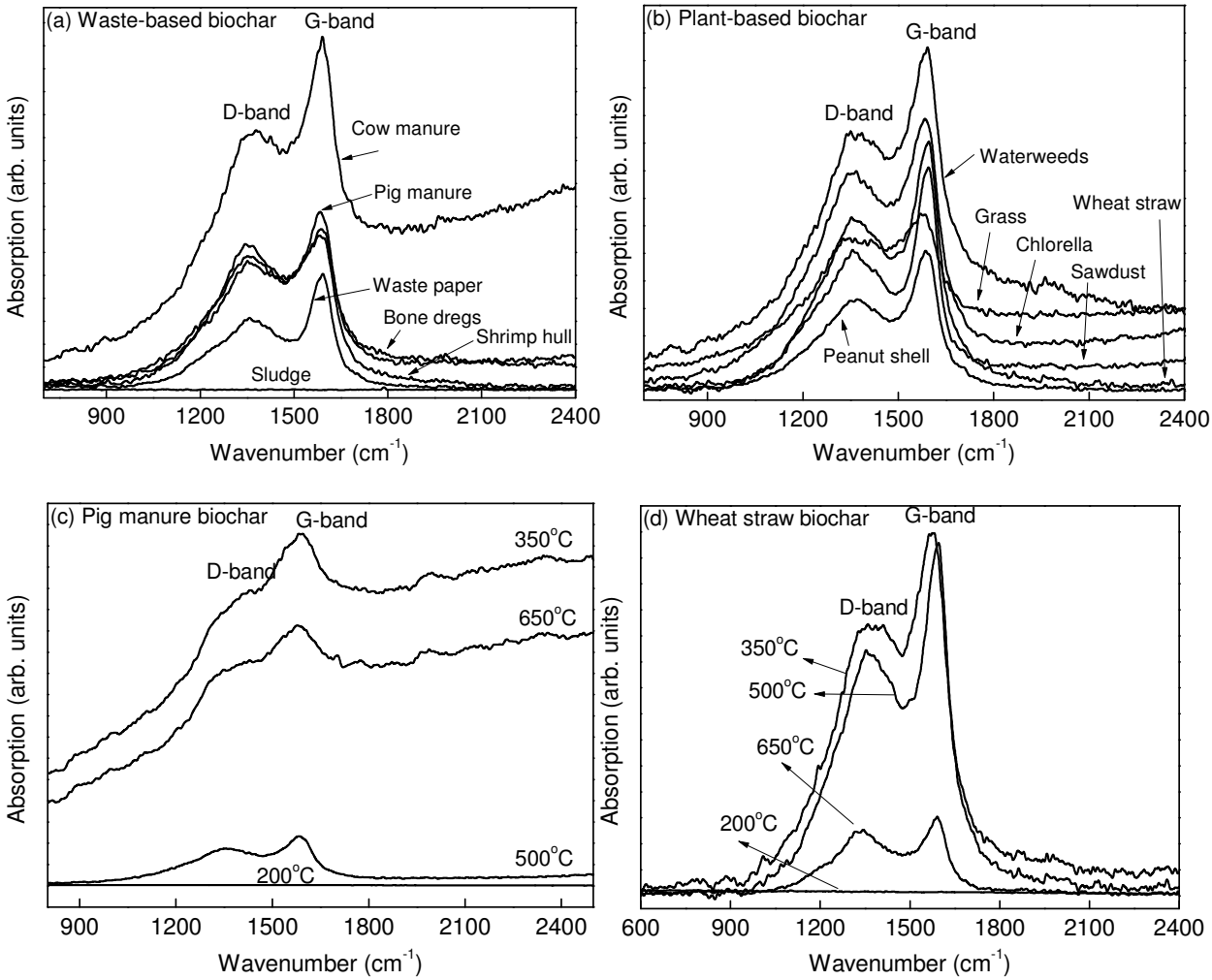

Fig. 4. Raman spectra of biochars derived from 12 feedstocks at 500°C (a, b) and biochars produced from pig manure (c) and wheat straw (d) at production temperature ranging 200°C–650°C.

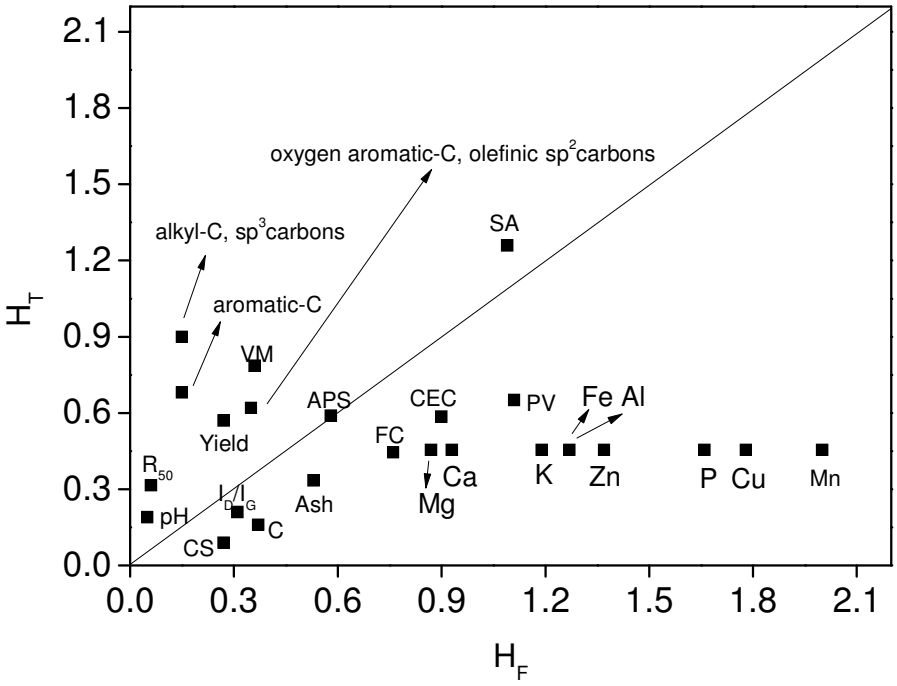

Fig. 5. Comparison of feedstock-depended heterogeneity (H_F) and temperature-depended heterogeneity (H_T) for different properties biochar.See Table 1 for abbreviation.